Article

Chinese Science Bulletin

Atmospheric Science

June 2011 Vol.56 No.18: 1921–1929
doi: 10.1007/s11434-011-4519-7

The quasi-biennial and semi-annual oscillation features of tropical O_3, NO_2, and NO_3 revealed by GOMOS satellite observations for 2002–2008

LIU Yi[1], LU ChunHui[1,2*], WANG Yong[1,2] & KYRÖLÄ Erkki[3]

[1] *Key Laboratory of Middle Atmosphere and Global Environment Observation, Institute of Atmospheric Physics, Chinese Academy of Sciences, Beijing 100029, China;*
[2] *Graduate University of the Chinese Academy of Sciences, Beijing 100049, China;*
[3] *Finnish Meteorological Institute, Earth Observation, Helsinki, Finland*

Received January 19, 2011; accepted March 25, 2011; published online May 12, 2011

The quasi-biennial oscillation (QBO) and semi-annual oscillation (SAO) characteristics of O_3, NO_2, and NO_3 from 2002 to 2008 were analyzed using Global Ozone Monitoring by Occultation of Stars (GOMOS) satellite observations. From investigations of the vertical and latitudinal structures of interannual anomalies for O_3 and the vertical velocity of the residual circulation (w-star), we conclude that dynamic transport is the principal factor controlling the QBO pattern of O_3. Under the influence of vertical transport, the QBO signals of O_3 originate in the middle stratosphere and propagate downward along with the w-star anomalies over the equator. The residual circulation has a significant role in tropical regions, regardless of altitude, while in extratropical regions, dynamic effects are important in some years in the lower stratosphere. In the middle stratosphere, dynamic transport is most efficient in the Southern Hemisphere. We also analyzed NO_2 anomalies and found that their QBO pattern was deep and stationary in the middle and upper stratosphere over the equator. This was due to the large depth over which w-star was anomalous. The latitudinal structure of NO_2 was asymmetric in extratropical areas in the middle stratosphere, but in the upper layers, the QBO pattern and dynamic influences were only observed in tropical zones. The interannual anomalies of NO_3 had an apparent SAO pattern in the tropical upper stratosphere because of different dynamic and chemical effects in different SAO phases. Chemical reactions may also have contributed to the QBO-type distribution of NO_2 and the SAO-type distribution of NO_3.

quasi-biennial oscillation, semi-annual oscillation, GOMOS satellite observation, stratospheric ozone, dynamic transport

Citation: Liu Y, Lu C H, Wang Y, et al. The quasi-biennial and semi-annual oscillation features of tropical O_3, NO_2, and NO_3 revealed by GOMOS satellite observations for 2002–2008. Chinese Sci Bull, 2011, 56: 1921–1929, doi: 10.1007/s11434-011-4519-7

The quasi-biennial oscillation (QBO) of stratospheric zonal wind and the semi-annual oscillation (SAO) of upper stratospheric zonal wind in equatorial regions have been widely investigated since they were discovered. Previous studies have searched for an underlying explanation of these oscillations [1,2], their influences on the global stratosphere [3], and their dynamic mechanism [4]. However, only a few investigations have analyzed the effects of the QBO and SAO using satellite observations. These studies focused on the distribution characteristics of the atmospheric components individually [5–9], but did not report on the relationship between the constituents and the dynamic effects of the oscillations.

The Global Ozone Monitoring by Occultation of Stars (GOMOS) stellar occultation instrument operates on ENVISAT, a sun-synchronous polar-orbiting satellite at approximately 800 km altitude and 98.55° inclination. GOMOS has provided long-term observation results from 2002 to 2008. These results offer a new perspective on the QBO and SAO. Some preliminary research was conducted on the distributions of O_3, NO_2, and NO_3 in 2003 using

*Corresponding author (email: alex61704@163.com)

these novel satellite data [10,11]. In a recent paper, Kyrölä et al. [12] showed the long-term variation in these distributions, proving the reliability of the new data. Recently, detailed analyses have been conducted on the variations in O_3, NO_2, and NO_3 and their responses to the QBO effects during 2002–2008 [13]. Furthermore, these satellite data were applied to investigate the dynamic formation of extreme ozone minimum events over the Tibetan Plateau [14].

1 Data and analysis

The measurement method employed by GOMOS makes it possible to obtain gas profiles accurately and precisely. Three spectral ranges are simultaneously observed by the GOMOS detector: 248–690 nm, 755–774 nm, and 926–954 nm. This makes it possible for GOMOS to retrieve vertical profiles of O_3, NO_2, NO_3, H_2O, O_2, and aerosols. The first three gases are discussed in this paper. The O_3 profiles have a vertical resolution of 2 km below 30 km and 3 km above 40 km. The NO_2 and NO_3 profiles have a vertical resolution of 3 km at any altitude. GOMOS fully covered the globe daily from 2002 to 2008, with the exception of July 2003 and January 2005, when there were problems with the steering system. Using an optimized code developed for the level 2 near-real-time analysis of GOMOS data, atmospheric vertical profiles of the concentrations of O_3, NO_2, and NO_3 were obtained in the middle atmosphere from 10 to 100 km. The GOMOS O_3 profiles were validated using ground-based and balloon sonde measurements. The differences between GOMOS and sonde measurements were typically positive. They were considered insignificant below 10%, particularly between 19 and 30 km, where biases were below 5% [15]. The profiles measured under dark limb conditions matched the ground-based measurements within ±2% for the altitude range 20–40 km [16].

The multi-year median distributions of zonal-average GOMOS mixing ratios for O_3, NO_2, and NO_3 are shown in Figure 1 to illustrate their climatological features. From these distributions, we determined that the three gases had similar characteristics. Specifically, the maximal centers of each distribution were all located in the equatorial stratosphere, but in different layers. O_3 reached approximately 30 km, with maximum values of 9 ppmv. NO_2 reached approximately 40 km, with maximum values of 14 ppbv, and NO_3 reached approximately 43 km, with maximum values of 250 pptv. Because the QBO and SAO are in different stratospheric layers, O_3, NO_2, and NO_3 are expected to be influenced by either the QBO or SAO in the middle atmosphere.

Temperature and wind fields derived from the European Centre for Medium-Range Weather Forecasts (ECMWF) ERA-Interim re-analysis data from 2002 to 2008 were also used to perform dynamic diagnostics. The ERA-Interim data had 37 vertical levels, with the top level at 50 km (1 hPa), and T159 spectral resolution [17]. Here we used a 240 ×121 (longitude vs. latitude) grid for the monthly mean data. Interannual anomalies were defined as the deviations in temperature and zonal wind from their respective 7-year means. Figure 2 shows the anomalies of zonal mean temperature and zonal wind in the equatorial stratosphere derived from the ECMWF results. These results show that both the wind and temperature fields had a conspicuous QBO cycle from the 100 to 5 hPa layers, and that these anomalies propagated from the upper to lower levels over time. Within the 5 to 1 hPa layers, significant SAO cycle signals were found in the wind and temperature fields. These signals had the same transformation phase. Compared with the distributions of the three studied gases, we found that O_3 was concentrated in the QBO region of 100 to 5 hPa

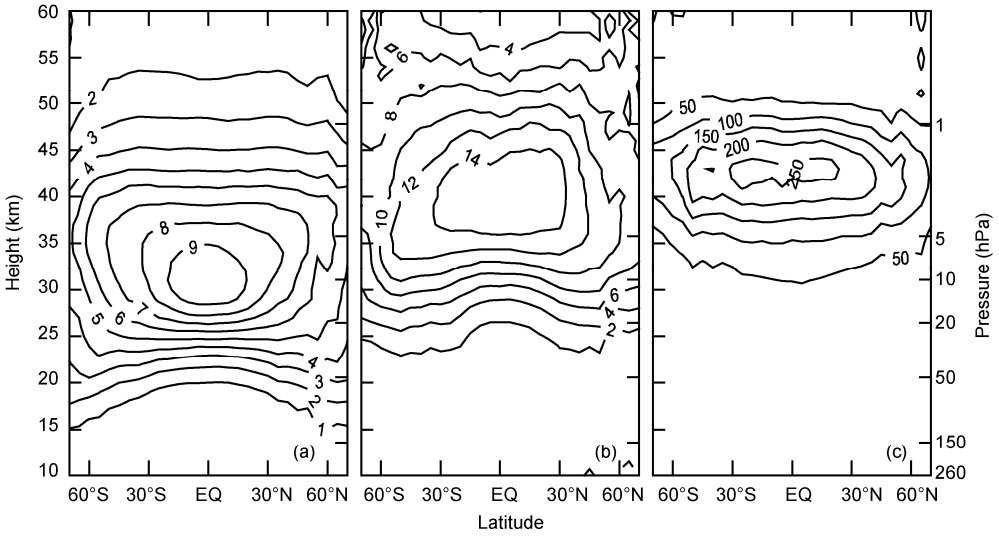

Figure 1 Meridional-vertical section of zonal mean GOMOS O_3, NO_2 and NO_3 concentrations. Data are median data from 2002 to 2008. (a) O_3 (ppmv); (b) NO_2 (ppbv); (c) NO_3 (pptv).

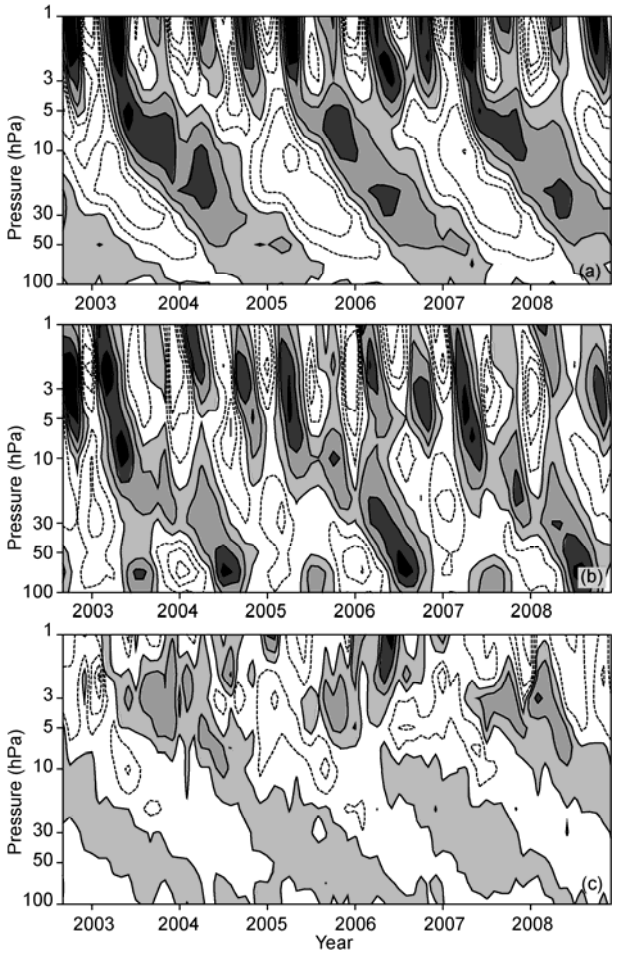

Figure 2 Equatorial zonal average time-vertical cross sections of (a) zonal wind anomalies with a contour interval of 10 m/s, (b) temperature anomalies with a contour interval of 2 K, and (c) w-star anomalies with a contour interval of 0.05 cm/s. Shaded areas indicate positive values.

and NO_3 was concentrated in the SAO region of 5 to 1 hPa. NO_2 concentrations overlapped parts of the QBO and SAO, suggesting that this species may have been affected by both dynamic processes.

2 O_3 and NO_2 QBO characteristics and dynamical analyses

Based on the above analyses, we investigated whether the QBO and SAO affected the distributions of O_3, NO_2, and NO_3 at different altitudes. Interannual anomalies were defined as the differences between the primitive data and the annual average of each month. Figure 3 shows the evolution of zonal averages of O_3 and NO_2 over time in the equatorial stratosphere, and Figure 3(a) presents the interannual anomalies of O_3. These graphs show that the oscillations occurred simultaneously in two layers in the middle and lower stratosphere. In the middle stratosphere, the layer was situated at 29 to 38 km and had the highest intensity of 1.5 ppmv. In the lower stratosphere, the layer was situated at 21 to 28 km and had lower intensity. To visualize the structure more clearly, we applied a 22- to 30-month band-pass filter to the O_3 interannual anomalies (Figure 3(b)) and defined the variance ratio as the ratio between the variance in filtered results and the variance in interannual anomalies, following the method of Shi et al. [18]. The variance ratio is shown in Figure 3(c). These results reveal that O_3 has typical QBO characteristics in most regions in the stratosphere. In the middle layers, the strongest QBO intensity reached 0.6 ppmv, with approximately 55% of the variance ratio explained by this correlation. In the lower layers, the QBO disturbed intensity also reached 0.6 ppmv, but there was a larger variance ratio that approached 60%. After analyzing the relationship between the O_3 anomalies and the QBO variations in different layers, we conclude that the zonal wind at 10 hPa (QBO proxy) and O_3 interannual anomalies underwent opposite phase changes in the middle stratosphere, but synchronous phase changes with a stronger QBO signal in the lower stratosphere. These variations in O_3 anomalies are attributed to differences in residual circulation (RC) between the western and eastern phases of the QBO.

The interannual anomalies of NO_2 and the 22- to 28-month band-pass filtered results of the anomalies are shown in Figure 3(d),(e). In these distributions, two layers of the QBO signals were observed in the middle and upper stratospheres (above 36 km), with the strongest oscillation magnitude reaching approximately 2 ppbv. After band-pass filtering, clearer QBO-type variances were observed with variance ratios of 40% to 60%. Compared with the O_3 variation, the QBO signals of NO_2 had the same transformation phase as zonal wind anomalies of 10 hPa.

To analyze the QBO features of O_3 and their relationships with the dynamic transport, time-height cross sections of the interannual anomalies for O_3 and w-star, the vertical velocity of the RC, are shown in Figures 3(a) and 2(c). The time series reveal the QBO as the dominant pattern of variability, with the largest centers of O_3 and w-star anomalies ($\approx$1.5 ppmv and 0.2 cm/s) being in the middle stratosphere (at around 32 km for O_3 and 3 hPa for w-star). The anomalies in O_3 and w-star originated almost simultaneously in the middle stratosphere and extended down gradually into the lower layers, with the same variation phase but opposite signs. Above an altitude of 28 km, positive O_3 anomalies corresponded to negative w-star anomalies. This result is explained by the upward transport under the downwelling regions; these two vertical motions converged around 10 hPa, which is the primary altitude of the O_3 distribution. This convergent vertical transport led to the positive O_3 anomalies above 28 km, and the anomalies propagated downward along with the negative w-star anomalies. When divergent vertical motions dominated at 10 hPa altitude because of upwelling above and downwelling below, O_3 anomalies were negative from 28 to 38 km. Hence, upward transport in the low layers brought in air with a low concen-

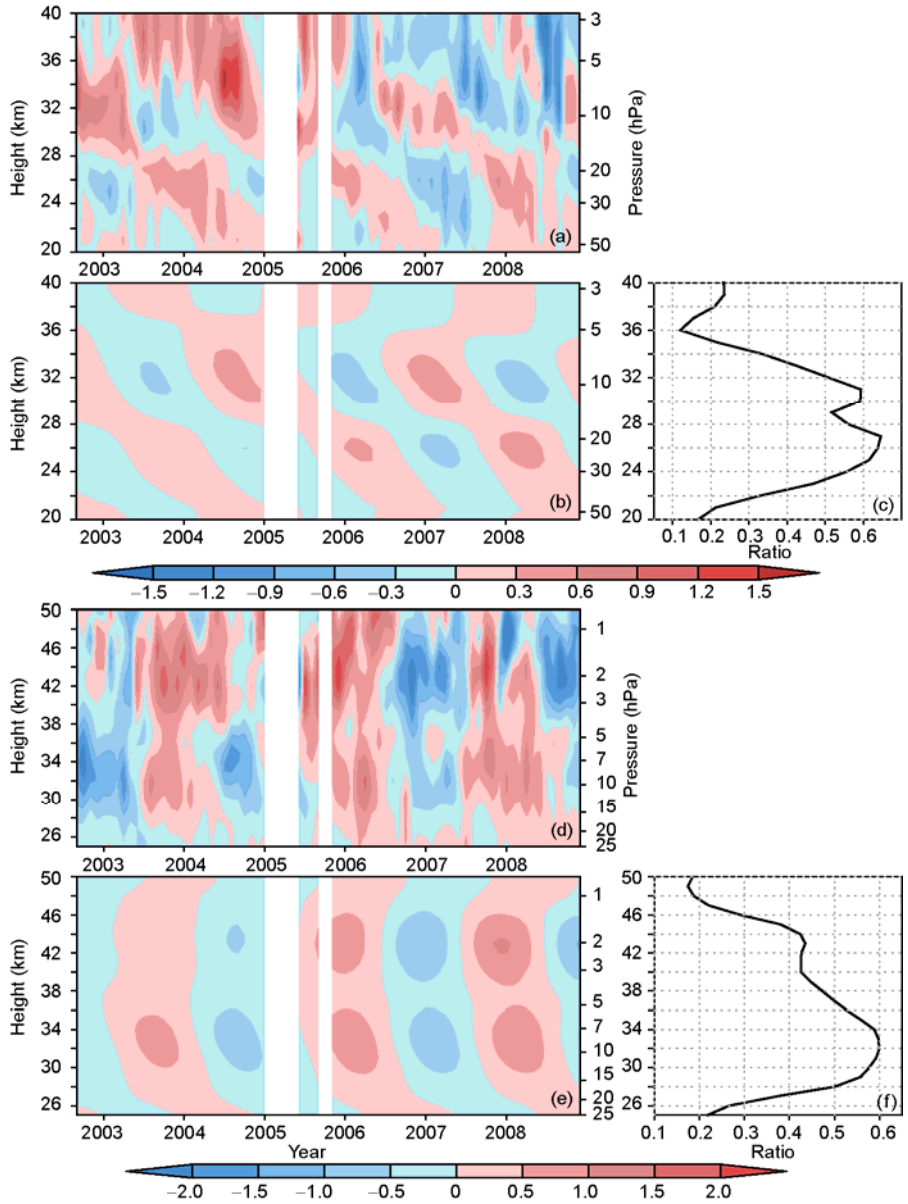

Figure 3 Equatorial zonal average time-vertical cross sections derived from GOMOS data for O_3 and NO_2. (a) Interannual anomalies of O_3 (ppmv); (b) 22–28-month band-pass filtered data of O_3 interannual anomalies; (c) the variance ratio of the QBO derived from the O_3 interannual anomalies; (d) interannual anomalies of NO_2 (ppbv); (e) 22–28-month band-pass data filtered of NO_2 interannual anomalies; (f) the variance ratio of the QBO derived from NO_2 interannual anomalies.

tration of O_3, resulting in the downward propagation of negative O_3 anomalies along with the positive w-star anomalies. These findings reveal that dynamic transport has a significant role in the vertical distribution of tropical O_3 interannual anomalies, covering not only the layers below 28 km mentioned by Hauchecorne et al. [13], but also the middle stratosphere (29–38 km).

Similarly, we compared the evolution of interannual anomalies for NO_2 (Figure 3(d)) and w-star in the equatorial stratosphere and concluded that dynamic transport was the leading factor for the QBO characteristics of NO_2. As discussed above, NO_2 was mainly distributed at an altitude of 40 km in the tropical stratosphere, which determined the importance of w-star between 3 and 5 hPa. When w-star was positive in these layers, air with a high concentration of NO_2 was transported into the upper stratosphere and mesosphere, leading to positive anomalies there (38–50 km). Under the upwelling areas, negative w-star anomalies could bring some NO_2 downward into the middle stratosphere (28–36 km), which also corresponded to positive centers of NO_2. The opposite vertical transport induced the opposite distribution of NO_2; negative w-star anomalies from 3 to 5 hPa altitude corresponded to negative NO_2 anomalies from 38 to 50 km. The upward transport in the lower layers may have brought air with a low concentration of NO_2, resulting in negative anomalies in the middle stratosphere. Anoma-

lous w-star values simultaneously dominated from 10 to 1 hPa, where NO_2 was mostly distributed. Hence, the QBO features of NO_2 were widely distributed over a range of heights in the middle and upper stratosphere and hardly propagated downward with time, in contrast to the case for O_3.

Time-latitude cross sections of O_3 anomalies at 26 km (Figure 4(a)), w-star anomalies at 20 hPa (Figure 4(b)), and NO_2 anomalies at 32 km (Figure 4(c)) reveal the latitudinal structure of the two species at the maximum QBO amplitude levels, along with the contribution from vertical dynamic transport. The w-star anomalies show the broad and symmetrical distribution of QBO variability around the equator, with upwelling in tropical areas and downwelling in extratropical regions or vice versa. The O_3 and NO_2 anomalies display evident QBO characteristics from 10°S to 10°N that were mainly controlled by dynamic transport. When w-star anomalies were negative at 20 hPa, the downward transport brought air with a high concentration of O_3 to the 26-km level, leading to positive anomalies of O_3 there. Similarly, ascending motion was able to transport air with a low concentration of NO_2 from lower levels to an altitude of 32 km, corresponding to negative anomalies of NO_2 there. When the vertical transport was in the opposite direction, the O_3 and NO_2 anomalies were also reversed. However, in the extratropical areas, O_3 anomalies did not perfectly correlate with the dynamic transport, and RC determined the meridional distributions of O_3 only in 2003, 2006, and 2008. Ascending motions in the tropical regions carried air with high O_3 concentration to the upper layers, and meridional transport carried this air to extratropical regions. Downward sections then transported this air to the lower stratosphere, increasing the concentration of O_3 at these levels. In some years, the distribution of O_3 may have been influenced by other factors, which require further investigation. In addition, the NO_2 anomalies exhibited an asymmetric structure in the extratropical stratosphere. In the Southern Hemisphere (SH), anomalous NO_2 corresponded well to the vertical transport. Low-concentration NO_2 air from the lower stratosphere propagated upward and decreased the content of NO_2 in the middle stratosphere. However, in the Northern Hemisphere (NH), NO_2 anomalies were inconsistent with the variation in w-star. This may have been due to the complexity of stratospheric circulations in NH extratropical areas. The westerly jet, deep convection, and planetary waves are all possible sources of the variation in the extratropical stratosphere; modeling studies are needed to draw conclusions that are more precise.

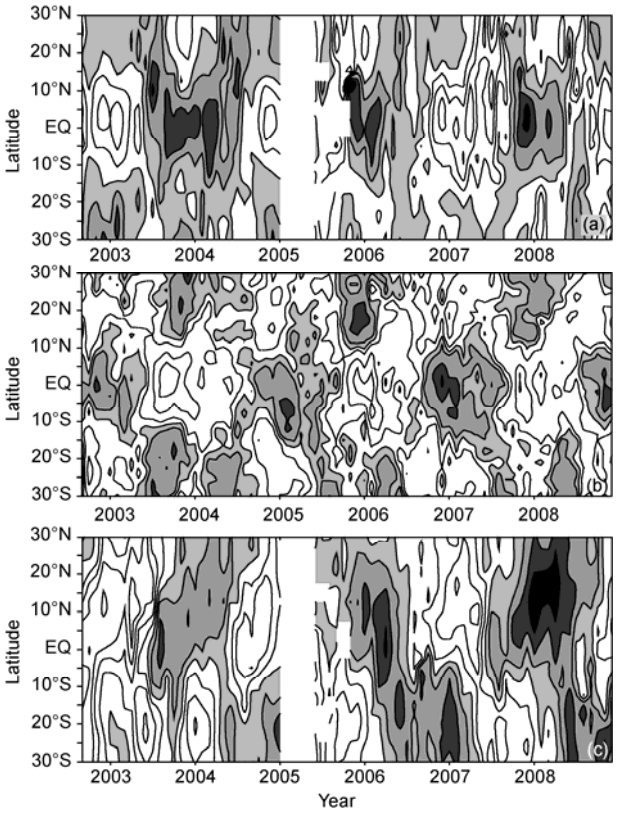

Figure 4 Time-latitude cross sections of (a) O_3 anomalies at 26 km with a contour interval of 0.2 ppmv, (b) w-star anomalies at 28 km (20 hPa) with a contour interval of 0.02 cm/s, and (c) NO_2 anomalies at 32 km with a contour interval of 0.5 ppbv. Shaded areas indicate positive anomalies.

We also investigated the latitudinal structures of O_3 (at 32 km) and NO_2 (at 42 km) anomalies at the levels of the second maximum QBO amplitudes, their relationship, and the w-star anomalies (not shown). In the middle stratosphere, O_3 anomalies showed an apparent QBO pattern in the tropical and SH extratropical regions, as did the distribution of NO_2 at 32 km (Figure 4(c)); dynamic transport had an important role in the O_3 distribution in these two areas. In the upper stratosphere, the QBO pattern of NO_2 anomalies was not as significant as that in the middle stratosphere, and the dynamics only influenced the tropical sections of the anomalous NO_2 data.

3 NO_3 SAO characteristics and dynamical/chemical diagnoses

According to the above analyses, we can summarize that the QBO is the primary factor driving the interannual anomalies of O_3 and NO_2 in the lower and middle stratosphere over the equatorial zone. The NO_3 deviations from the 6-year (2003–2008) mean were defined as interannual anomalies. Time-height cross sections of the NO_3 anomalies are shown in Figure 5(a). These reveal that the SAO was the dominant pattern of variability, with the largest center (100 pptv) being in the upper stratosphere around 42 km. The oscillation phases of NO_3 were synchronous with the wind anomalies of 2 hPa (SAO proxy). After 4 to 8 months of band-pass filtering, the variance ratios of SAO signals exceeded 60%, with the largest value being 75% at an altitude of 44 km.

It is well known that the lifetime of NO_3 is shorter than those of O_3 and NO_2, with high sensitivity to temperature [19]. It is therefore not surprising to observe that the SAO

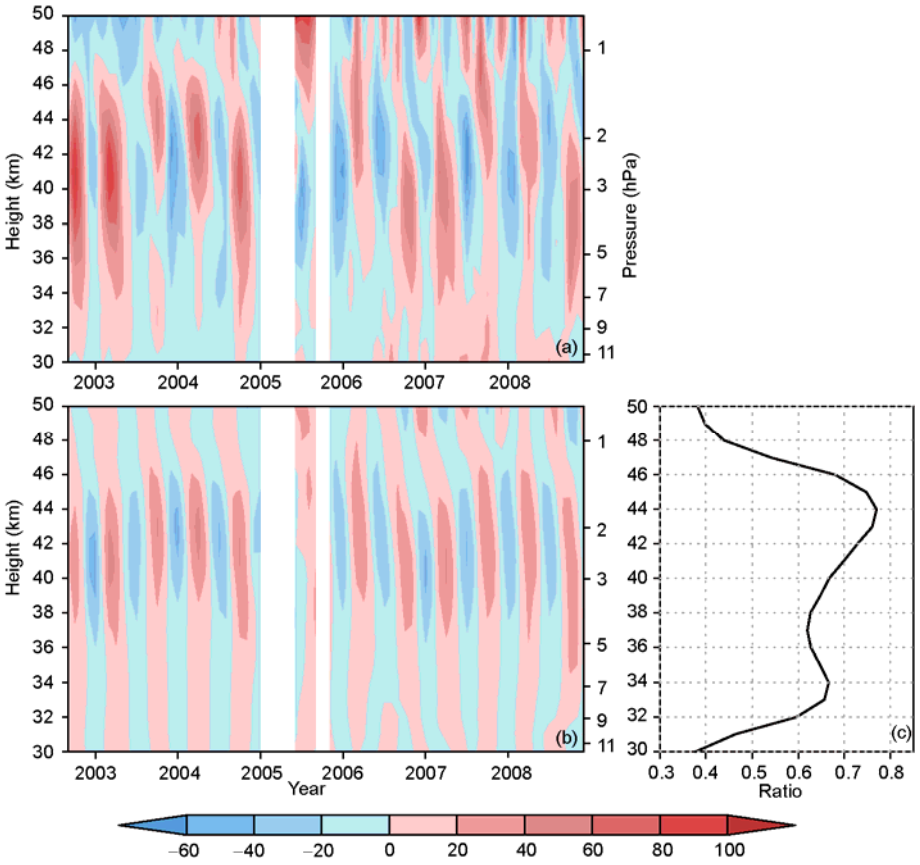

Figure 5 Equatorial zonal average time-vertical cross section derived from GOMOS data for NO_3. (a) Interannual anomalies of NO_3 (pptv); (b) 4–8-month band-pass filtered data of NO_3 interannual anomalies; (c) the variance ratio of the SAO derived from NO_3 interannual anomalies.

pattern of NO_3 anomalies was closely correlated with the SAO characteristics of ECMWF temperatures (Figure 2(b)) in the upper stratosphere. In addition, Marchand et al. [19] supposed that the chemical equilibrium of NO_3 was controlled by the chemical reaction among NO_2, O_3, and NO_3, which strongly depended on positive temperature:

$$NO_2 + O_3 \rightarrow NO_3 + O_2 \quad (1)$$

Hence, NO_3 anomalies chiefly exhibit SAO characteristics, and the chemical effect is a contributing factor.

Dynamical influences are also important in the SAO variation in NO_3 anomalies. Composite distributions of RC deviations from the 6-year mean in the western and eastern phases of the SAO are shown in Figure 6(a),(b). In the western phase of the SAO, we clearly observe two meridional circulations in the upper stratosphere: a counterclockwise cell in the NH and a clockwise cell in the SH. These two circulations induced intense downward transport in the equatorial upper stratosphere from 10 to 1 hPa. They brought air with high NO_3 concentration to these levels from the upper atmosphere, corresponding to the positive NO_3 anomalies. Furthermore, adiabatic descending motion induced positive temperature anomalies, which also increased the NO_3 levels. In contrast, these two meridional circulations had opposite propagation directions in the eastern phase of the SAO, moving clockwise in the NH and counterclockwise in the SH. This huge transformation resulted in the low-concentration NO_3 air from the lower stratosphere replacing the original high-concentration air in the 10 to 2 hPa layers. Ascending motion also induced negative temperature anomalies. Both these factors reduced the NO_3 concentration, as shown by the blue regions in Figure 5(a).

The above analyses indicate that the QBO has an apparent influence on the distributions of O_3 and NO_2, mainly because of dynamic processes, while the SAO influences NO_3 anomalies both dynamically and chemically. To identify concrete chemical and dynamic influences, we examined the correlation coefficients of correlation between O_3, NO_2, and NO_3 interannual anomalies and QBO and SAO proxies (Figure 7). The equatorial zonal wind at 10 hPa served as a QBO proxy, and the wind at 2 hPa served as an SAO proxy. In the case of the QBO effects, we find that most influences were concentrated in the lower and middle stratosphere. The O_3/QBO ratio had two high-value areas, with a shift at 28 km, similar to the distribution shown in Figure 3. Previous studies indicated the existence of a transition between the dynamic control of O_3 below 28 km and a chemical/temperature control above 28 km [20,21]. Consequently, the correlation coefficients and variance ratios of

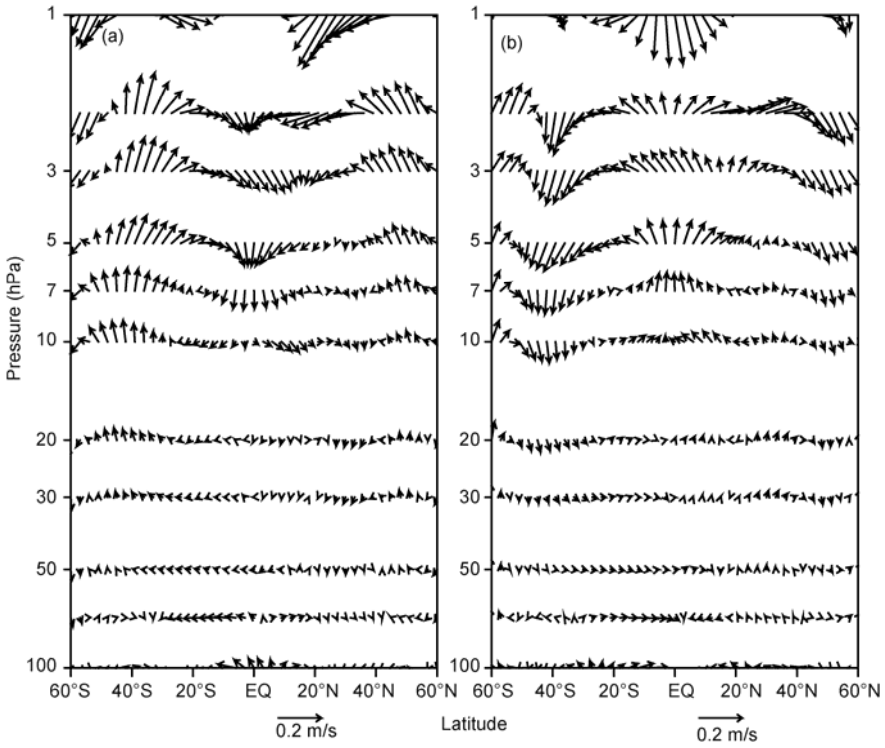

Figure 6 Composite RC anomalies in different phases of the SAO derived from ERA-Interim/ECMWF data, where the quiver unit is m/s: (a) the western phase of the SAO; and (b) the eastern phase of the SAO.

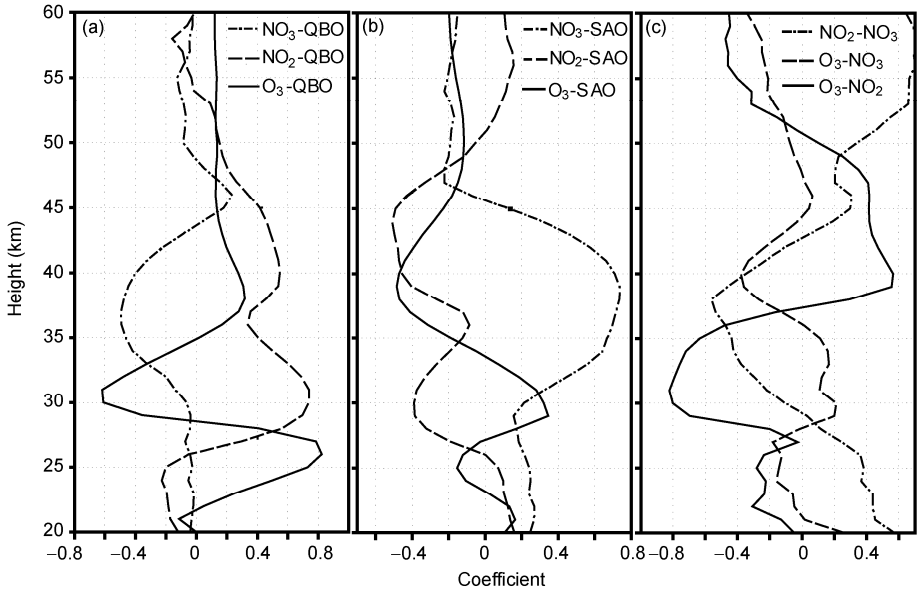

Figure 7 Coefficients of correlation between the interannual anomalies of (a) O_3, NO_2, NO_3 and the QBO proxy (zonal wind at 10 hPa); (b) O_3, NO_2, NO_3 and the SAO proxy (zonal wind at 2 hPa); and (c) O_3, NO_2 and NO_3 mixing ratios.

O_3/QBO (Figure 3(c)) were higher in the lower stratosphere and lower in the upper stratosphere. The correlation of NO_2/QBO has two positive regions: one from 28 to 35 km and one from 37 to 45 km, as in Figure 3. These are related to the chemical reactions and dynamic transport. In the case of NO_3/QBO, there was an area of negative correlation around 36 km owing to vertical transport in different phases of the QBO.

In terms of the SAO influence, the NO_3/SAO correlation presented a succession of positive regions ranging in altitude from 30 to 45 km. These positive regions resulted from meridional circulation in different phases of the SAO. The O_3/SAO correlation had a succession of negative areas around 40 km, and the NO_2/SAO correlation had negative

values from 30 to 47 km, unlike the correlation with NO_3. This was because the main areas of the O_3 and NO_2 distributions were lower than those of the NO_3 distribution, and therefore, the same transport direction would have brought different types of air. Thus, the ascending transport either supplied the air with high concentrations of O_3 and NO_2 but low concentrations of NO_3, or with high concentrations of NO_3 but low concentrations of O_3 and NO_2.

There were three remarkable regions where the absolute values of coefficients of correlation among O_3, NO_2, and NO_3 were larger than 0.5. First, there was negative correlation between O_3 and NO_2 between 28 and 35 km. This region was a result of the catalytic destruction of O_3 by NO_x [22]. Second, the correlation between O_3 and NO_2 was positive between 38 and 48 km. Third, NO_2 and NO_3 correlation was positive between 50 and 60 km. Hauchecorne et al. [13] proposed possible explanations for the first two findings. However, most observational studies have been limited to altitudes below 40 km and could not capture the third feature; therefore, we investigated the possible explanations. In the equatorial region, there was a significant amount of N_2O in the upper stratosphere [23]. Vertical motion may have brought more N_2O into the upper layers, increasing the production of NO_x from N_2O oxidation with atomic oxygen. This mechanism would have supplied sufficient NO_2 to these levels and enabled chemical reaction (1) between NO_2 and NO_3. This reaction has a strong positive temperature dependence and is prevalent in the upper stratosphere [24]. Further model and observational studies are needed to test this hypothesis and to better understand the mechanisms involved. The O_3 and NO_3 correlation is difficult to study because O_3 undergoes its own chemical reactions in the upper stratosphere, such as the O_3 loss reaction

$$2O_3 + O_2 \rightarrow 4O_2 \quad (2)$$

of the Chapmen cycle, which also has strong temperature dependence [24].

As discussed above, dynamic control of the QBO is the most influential factor for O_3 and NO_2 concentrations. Between 32 and 45 km, the dynamic effects of the SAO significantly influenced the distribution of NO_3, and chemical reaction was the other important driver of concentrations at these levels. Furthermore, complicated chemical reactions in the upper stratosphere can influence the correlation between NO_2 and NO_3.

4 Discussion and conclusion

The concentrations of stratospheric species O_3, NO_2, and NO_3 were measured in GOMOS observations during 2002–2008. These observations made it possible to investigate the interannual evolution of the atmospheric composition, which can improve our understanding of atmospheric variations. We analyzed the responses of O_3, NO_2, and NO_3 concentrations to QBO and SAO variations, and examined the reasons for these distribution patterns from dynamic and chemical perspectives.

We focused on the overall results obtained from GOMOS observations and ERA-Interim re-analysis data. First, we found that the distributions of O_3 interannual anomalies had significant QBO-type characteristics, which were closely associated with the stratospheric zonal wind anomalies caused by the QBO phenomenon over equatorial areas. Moreover, from analyses of the vertical distributions of O_3 and w-star over the equator, we found that dynamic transport was the leading factor influencing equatorial O_3 anomalies. The operating ranges covered 20 to 38 km, including the layers below 28 km that were studied by Hauchecorne et al. [13]. In addition, latitudinal structures in the low and middle stratosphere indicated that dynamic effects have a significant role in tropical areas (10°S–10°N), regardless of altitude, while in extratropical regions, dynamic transport was effective in a few years in the lower stratosphere and more efficient in the SH in the middle stratosphere. Second, the vertical distributions of NO_2 showed that the QBO pattern dominated in the middle and upper stratosphere and hardly propagated downward with time. This was attributed to the wide height distribution of anomalous w-star values from 10 to 1 hPa. In addition, the NO_2 anomalies had an asymmetric structure in extratropical areas of the middle stratosphere, but they corresponded well to vertical transport in the SH. In the upper stratosphere, the QBO pattern was not conspicuous to explain anomalies, and dynamic effects were effective only in tropical zones. Third, SAO-type traits of NO_3 interannual anomalies were clearly observed in the upper stratosphere (10 to 1 hPa). By analyzing the distributions of RC anomalies in the eastern and western SAO, we confidently conclude that dynamic effects were significant for these distribution patterns. Vertical motions in the equatorial stratosphere not only transported air with high- or low-concentration NO_3, but also affected temperature, which can determine the chemical reaction of NO_3 formation. Finally, chemical reactions are of great importance to the atmospheric constituents in the upper stratosphere and lower mesosphere. Our dynamic diagnoses (RC) included variations in atmospheric fields, wind and temperature, as well as the influence of temperature disturbance on chemical reactions. Accordingly, further model and observational investigations are needed to distinguish dynamic and chemical effects.

In summary, many factors can affect the long-term evolution of the atmospheric composition. In this study, we explored two factors: chemical reactions and zonal wind anomalies resulting from the QBO and SAO phenomena. Detailed analyses of the evolutional characteristics of stratospheric constituents because of dynamic and chemical processes will help us further understand both stratospheric variations and their influences on constituent changes in the atmosphere.

This work was supported by the National Basic Research Program of China (*2010CB428604*), *Dragon 2 Program* (*ID:5311*) *and the National Natural Science Foundation of China* (*40633015*). *The meteorological analysis was kindly provided by ECMWF.*

1 Wallace J M, Holton J R. A diagnostic numerical model of the quasi-biennial oscillation. J Atmos Sci, 1968, 25: 280–292
2 Wallace J M, Panetta R L, Estberg J. Representation of the equatorial stratospheric quasi-biennial oscillation in EOF phase space. J Atmos Sci, 1993, 50: 1751–1762
3 Holton J R, Tan H C. The influence of the equatorial quasi-biennial oscillation on the global circulation at 50 mb. J Atmos Sci, 1980, 37: 2200–2208
4 Plumb R A. The interaction of two internal waves with the mean flow: Implications for the theory of the quasi-biennial oscillation. J Atmos Sci, 1977, 34: 1847–1858
5 Tung K, Yang H. Global QBO in circulation and ozone, part I, reexamination of observational evidence. J Atmos Sci, 1994, 51: 2699–2707
6 Tung K, Yang H. Global QBO in circulation and ozone, part II, a simple mechanistic model. J Atmos Sci, 1994, 51: 2708–2721
7 Logan J A, Jones D B, Megretskaia I A, et al. Quasi-biennial oscillation in tropical ozone as revealed by ozone-sonde and satellite data. J Geophys Res, 2003, 108: 4244, doi: 10.1029/2002JD002170
8 Chen Y J, Zheng B, Zhang H. The features of ozone quasi-biennial oscillation in tropical stratosphere and its numerical simulation. Adv Atmos Sci, 2002, 19: 777–793
9 Zheng B, Shi C H, Chen Y J. Anti-symmetric transport of middle stratospheric methane with respect to the equator. Chinese Sci Bull, 2006, 51: 1761–1765
10 Kyrölä E, Tamminen J, Leppelmeier G W, et al. Nighttime ozone profiles in the stratosphere and mesosphere by the global ozone monitoring by occultation of stars on envisat. J Geophys Res, 2006, 111: D24306, doi: 10.1029/2006JD007193
11 Hauchecorne A, Bertaux J L, Dalaudier F, et al. First simultaneous global measurements of nighttime stratospheric NO_2 and NO_3 observed by global ozone monitoring by occultation of stars in 2003. J Geophys Res, 2005, 110: D18301, doi: 10.1029/ 2004JD005711
12 Kyrölä E, Tamminen J, Sofieva V. Gomos O_3, NO_2, and NO_3 observations in 2002–2008. Atmos Chem Phys, 2010, 10: 7723–7738
13 Hauchecorne A, Bertaux J, Dalaudier F, et al. Response of tropical stratospheric O_3, NO_2 and NO_3 to the equatorial quasi-biennial oscillation and to temperature as seen from Gomos/Envisat. Atmos Chem Phys, 2010, 10: 8873–8879
14 Liu C X, Liu Y, Cai Z N, et al. A Madden-Julian oscillation triggered record ozone minimum over the Tibetan Plateau in December 2003 and its association with stratospheric "low-ozone pockets". Geophys Res Lett, 2009, 36: L15830, doi: 10.1029/2009GL039025
15 Liu Y, Cai Z N, Kyrölä E. Comparison of Envisat Gomos and Mipas ozone profiles with balloon sonde measurements from Beijing. Proc Dragon Program Final Results 2004–2007, 2008
16 Van Gijsel J, Swart D, Baray J, et al. Gomos ozone profile validation using ground-based and balloon sonde measurements. Atmos Chem Phys Discuss, 2010, 10: 8515–8551
17 Dee D, Uppala S. Variational bias correction of satellite radiance data in the Era-interim reanalysis. Quart J R Meteorol Soc, 2009, 135: 1830–1841
18 Shi C H, Zheng B, Chen Y J, et al. The quasi-biennial oscillation of water vapor in tropical stratosphere (in Chinese). Chin J Geophys, 2009, 52: 2428–2435
19 Marchand M, Bekki S, Lefevre F, et al. Temperature retrieval from stratospheric O_3 and NO_3 Gomos data. Geophys Res Lett, 2007, 34: L24809, doi: 10.1029/2007GL030280
20 Butchart N, Scaife A, Austin A, et al. Quasi-biennial oscillation in ozone in a coupled chemistry-climate model. J Geophys Res, 2003, 108: 4486, doi: 10.1029/2002JD003004
21 Tian W S, Chipperfiled M, Gray L, et al. Quasi-biennial oscillation and tracer distributions in a coupled chemistry-climate model. J Geophys Res, 2006, doi: 10.1029/2005JD006871
22 Chipperfield M, Gray L, Kinnersley J, et al. A two-dimensional model study of the qbo signal in Sage NO_2 and O_3. Geophys Res Lett, 1994, 21: 589–592
23 Jin J J, Semeniuk K, Beagley S, et al. Comparison of cmam simulations of carbon monoxide (CO), nitrous oxide (N_2O), and methane (CH_4) with observations from Odin/Smr, Ace-Fts, and Aura/Mls. Atmos Chem Phys, 2009, 9: 3233–3252
24 Brasseur G P, Solomon S. Aeronomy of the Middle Atmosphere: Chemistry and Physics of the Stratosphere and Mesosphere. 3rd ed. Heidelberg: Springer, 2005